Inorganic Chemistry

Article

pubs.acs.org/IC

Semiconductive and Magnetic One-Dimensional Coordination Polymers of Cu(II) with Modified Nucleobases

Pilar Amo-Ochoa,*[,†] Oscar Castillo,[‡] Carlos J. Gómez-García,[§] Khaled Hassanein,[†] Sandeep Verma,*[,∥] Jitendra Kumar,[∥] and Félix Zamora*[,†]

[†]Departamento de Química Inorgánica, Universidad Autónoma de Madrid, 28049 Madrid, Spain

[‡]Departamento de Química Inorgánica, Universidad del País Vasco (UPV/EHU), Apartado 644, E-48080 Bilbao, Spain

[§]Instituto de Ciencia Molecular (ICMol), Parque Científico, Universidad de Valencia, Catedrático José Beltrán, 2, 46980 Paterna Valencia, Spain

[∥]Department of Chemistry, Indian Institute of Technology Kanpur, Kanpur-208016 (UP), India

Supporting Information

ABSTRACT: Four new copper(II) coordination complexes, obtained by reaction of CuX_2 (X = acetate or chloride) with thymine-1-acetic acid and uracil-1-propionic acid as ligands, of formulas $[Cu(TAcO)_2(H_2O)_4]\cdot 4H_2O$ (**1**), $[Cu(TAcO)_2(H_2O)_2]_n$ (**2**), $[Cu_3(TAcO)_4(H_2O)_2(OH)_2]_n\cdot 4H_2O$ (**3**), and $[Cu_3(UPrO)_2Cl_2(OH)_2(H_2O)_2]_n$ (**4**) (TAcOH = thymine-1-acetic acid, UPrOH = uracil-1-propionic acid) are described. While **1** is a discrete complex, **2**−**4** are one-dimensional coordination polymers. Complexes **2**−**4** present dc conductivity values between 10^{-6} and 10^{-9} S/cm^{-1}. The magnetic behavior of complex **2** is typical for almost isolated Cu(II) metal centers. Moderate−weak antiferromagnetic interactions have been found in complex **3**, whereas a combination of strong and weak antiferromagnetic interactions have been found in complex **4**. Quantum computational calculations have been done to estimate the individual "*J*" magnetic coupling constant for each superexchange pathway in complexes **3** and **4**. Compounds **2**−**4** are the first known examples of semiconductor and magnetic coordination polymers containing nucleobases.

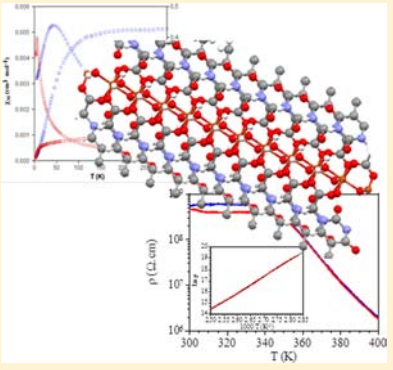

INTRODUCTION

DNA nanotechnology provides one of the most interesting approaches to form tailored complex structures with precise control over molecular features.[1] However, its intrinsic electrical conductivity does not give the basis for electronic functions. The DNA molecule needs to be functionalized with electronic materials in order to increase its electrical conductivity and to assemble functional electronic devices. The ability of nucleic acid arrays to arrange other molecules allows potential applications in molecular-scale electronics since the assembly of a nucleic acid lattice may template the assembly of molecular electronic elements such as molecular wires. The nucleic acid nanostructures could provide a method for nanometer-scale control of the placement and overall architecture of these components, essentially using nucleic acid structures as a molecular breadboard. DNA has been mainly used as a template upon which to organize more highly conductive materials such as (i) metal clusters on DNA,[2,3] (ii) metallization (electrostatic binding of metal ions and reduction),[4] (iii) formation of metallic-DNA (insertion of metal ions by coordination between complementary nucleobases on DNA),[2] and (iv) decoration of DNA with semiconducting or surface-functionalized metal nanoparticles.[5] Coordination polymers (CPs) have attracted remarkable attention in recent years from structural and properties viewpoints.[6] In particular most of the studies have been focused on aspects related to their porosity, large inner surface area, tunable pore sizes, and topologies,[7] leading to various architectures[8] and promising applications[9,10] such as gas adsorption[11] and storage,[12] heterogeneous catalysis,[13] nanoparticles,[14] luminescence,[15] nonlinear optics,[16] magnetism,[17] and electrical conductivity.[18] Recently, a breakthrough pointed out the potential use of 1D-CPs as molecular nanowires thanks to the excellent conductivity values reported for some nanostructures of these compounds.[19−21]

Our approach tries to combine the molecular recognition capability of the DNA with the (multi)functional properties of certain coordination polymers. We plan to form (multi)-functional 1D coordination polymers containing nucleobases and then connect those polymers to selected sequences of oligonucleotides. The self-assembly between the DNA and the coordination polymer will produce new nanohybrid materials with new interesting properties with the feasibility of using well-known DNA structural capabilities, including origami DNA, toward complex nanocircuit formation.

Despite the importance of these potential applications as advanced functional materials, the scarce studies with one-

Received: July 8, 2013
Published: September 16, 2013

   dx.doi.org/10.1021/ic401758w | *Inorg. Chem.* 2013, 52, 11428−11437

dimensional and high dimensional polymeric nucleobase structures have primarily focused on biological and biomimetic aspects or in the construction of new metal organic frameworks.[22−37]

Surprisingly, the study of one-dimensional coordination polymers with nucleobases exhibiting magnetic or conductive properties is also very scarce.[38] With the aim to extend the potential of these compounds to the fabrication of complex conductive structures, we have explored the idea to use CPs containing nucleobases[39,40] with basic structural aspects resembling those expected for M-DNA.[39] The results obtained, although promising, suggest that new systems have to be prepared to improve their electrical properties.

On the basis of these principles, as a first step we focus on the design and synthesis of one-dimensional (1D) coordination polymers with selected transition metals and modified nucleobases in order to study their electrical and magnetic properties. We have selected carboxylic functionalized nucleobases, (i) thymine-1-acetic acid (TAcOH) and (ii) uracil-1-propionic acid (UPrOH), which are excellent candidates to coordinate to Cu(II) *via* the carboxylate group (Figure 1). This metal ion could provide the material with interesting magnetic or electrical properties.[18] The direct reactions between the two building blocks, metal ion and nucleobases, has allowed us to isolate three unprecedented 1D coordination polymers of Cu(II)-containing nucleobases. Herein, we present their structural, magnetic, and electrical studies.

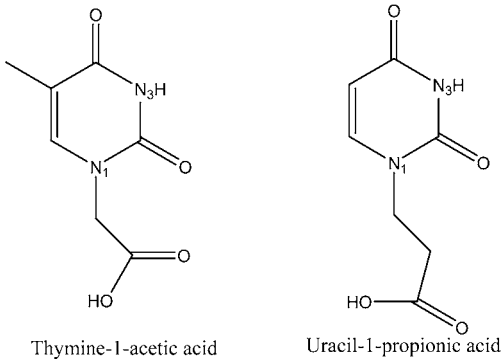

Figure 1. Schematic representation of the thymine-1-acetic acid (TAcOH) (left) and the uracil-1-propionic acid (UPrOH) (right).

EXPERIMENTAL SECTION

Materials and Methods. Copper(II) acetate monohydrate, copper(II) chloride, thymine-1-acetic acid, uracil, N-methyl imidazole, and other chemicals were purchased from standard chemical suppliers and used as received. IR spectra were recorded on a PerkinElmer spectrum 100 spectrophotometer using a universal ATR sampling accessory and on a Bruker FT-IR Vector 22 model from 4000 to 400 cm^{-1} as KBr pellets. Elemental analyses were carried out by the Microanalytical Service of the Autónoma University of Madrid and on a Thermoquest CE instrument CHNS-O elemental analyzer (Model EA/10) at IIT Kanpur. ^{1}H and ^{13}C NMR spectra were recorded either on a JEOL-JNM LAMBDA 400 model operating at 400 and 100 MHz, respectively, or on JEOL ECX-500 model operating at 500 and 125 MHz, respectively. The chemical shifts were referenced with respect to tetramethylsilane. The high resolution mass spectra [HRMS] were recorded in a Q-Tof Premier Micromass HAB 213 mass spectrometer using a capillary voltage of 2.6−3.2 kV. L-SIMS spectra were obtained with a Waters/Autospec mass spectrometer, using m-NBA (m-nitrobenzyl alcohol) as a matrix. Peak identifications were based on the *m*/*z* values and the isotopic distribution patterns.

Powder X-ray diffraction has been done using a Diffractometer PANalyticalX'Pert PRO theta/2theta primary monochromator and detector with fast X'Celerator. The samples have been analyzed with scanning theta/2theta.

Preliminary direct current (DC) electrical conductivity measurements were performed on two different single crystals of compounds **2** and **3** and in two different pellets for compound **4**, with carbon paint at 300 K and two contacts. The contacts were made with platinum wires (25 μm diameter). The samples were measured at 300 K applying an electrical current with voltages form +10 to −10 V. The measurements were performed in the compounds along the crystallographic *a* axis.

The DC electrical conductivity measurements were carried out also with the four contacts method on two single crystals of compound **2** and four of compound **3** in the temperature range 300−400 K since the resistance at room temperature exceeded the detection limit of our equipment (5×10^{11} Ω), precluding its study at low temperatures. The contacts were made with Pt wires (25 μm diameter) using graphite paste. The samples were measured in a Quantum Design PPMS-9 equipment connected to an external voltage source (Keithley model 2400 source-meter) and amperometer (Keithley model 6514 electrometer). All the conductivity quoted values have been measured in the voltage range where the crystals are Ohmic conductors. All the measured crystals showed similar conductivity values and thermal behaviors. The cooling and warming rates were 0.5 and 1 K/min, and the results were similar in the cooling and warming scans.

Magnetic measurements were performed on polycrystalline samples of the complexes taken from the same uniform batches used for the structural determinations with a Quantum Design MPMS-XL5 SQUID susceptometer in the temperature range 5−300 K with an applied magnetic field of 5000 G. The susceptibility data were corrected for the sample holder previously measured using the same conditions and for the diamagnetic contribution of the salt as deduced by using Pascal's constant tables.[41]

The X-ray diffraction data collections and structure determinations were done at 100(2) K on an Oxford Diffraction Xcalibur diffractometer. All the structures were solved by direct methods using the SIR92 program[42] and refined by full-matrix least-squares on F^2 including all reflections (SHELXL97).[43] All calculations were performed using the WINGX crystallographic software package.[44] All non-hydrogen atoms were refined anisotropically. The hydrogen atoms of the 3-(1-uracilyl)propanoate and thyminyl ligands were either positioned geometrically and allowed to ride on their parent atoms or located at the Fourier difference map and fixed at that position (hydroxyl and water O−H). Crystal parameters and details of the final refinements of compounds **1**−**4** are summarized in Table S1.

For complex **4**, the water and hydroxide hydrogen atoms were located on a Fourier map; however constraints were applied to fix the O−H distance and H−O−H angle.

Syntheses. *Synthesis of Ethyl-3-(1-uracilyl)propanoate.* Uracil (10 g, 89.2 mmol) and ethyl acrylate (13.4 mL, 125.8 mmol) were suspended in 150 mL of dry DMF, and N-methylimidazole (1.0 mL) was added. The white reaction mixture was stirred under a N_2 atmosphere for 18 h (color changes from white to colorless). The completion of the reaction was monitored by TLC analysis. The solvent was evaporated under reduced pressure, affording an oily product. To the residue was added 50 mL of diethyl ether and sonicated for 10 min. The resulting suspension was cooled at 0 °C overnight to induce precipitation. The precipitate was filtered and dried to afford the desired product as a white powder (16.0 g, 85% yield). HRMS $(M + Na)^+$ calculated: 235.07. Found: 235.07. M.P. 114−116 °C. ^{1}H NMR (400 MHz, $CDCl_3$, 25 °C, TMS): δ (ppm) 1.17 (t, 3H, CH_3), 2.71 (t, 2H, CH_2), 3.94 (t, 2H, CH_2), 4.07 (q, 2H, CH_2), 5.61 (d, 1H, C5−H), 7.36 (d, 1H, C6−H), 10.25 (broad, 1H, N3−H). ^{13}C NMR (100 MHz, $CDCl_3$, 25 °C, TMS): δ (ppm) 13.93, 32.86, 45.07, 60.92, 101.60, 145.67, 150.95, 164.166, 171.21. Anal. Calcd (found) for $C_9H_{12}N_2O_4$: C, 50.94 (52.36); H, 5.70 (5.59); N, 13.20 (13.67).

Synthesis of 3-(1-uracilyl)propanoic Acid (UPrOH). The above ester (2.0 g, 9.4 mmol) was suspended in 40 mL of 5 M HCl and

dx.doi.org/10.1021/ic401758w | *Inorg. Chem.* 2013, 52, 11428−11437

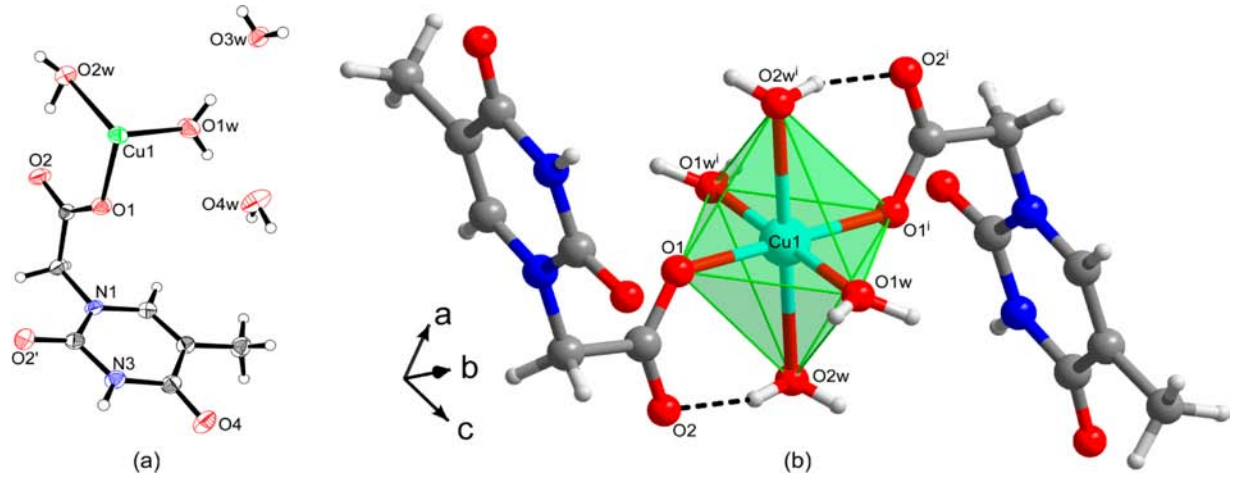

Figure 2. (a) ORTEP representation of the asymmetric unit of complex **1** at the 35% probability level. (b) Complex entity found in compound **1** with coordination polyhedron around the Cu center (C, gray; H, light gray; N, blue; O, red; Cu, turquoise).

refluxed for 10 h. The reaction mixture was cooled to room temperature and then neutralized with Na_2CO_3 up to pH 6. The solution was concentrated under reduced pressure to 20 mL, and DMF (20 mL) was added to precipitate the sodium chloride salt. The DMF layer was cooled to 0 °C for 1 h and filtered. Then, the filtrate was evaporated under reduced pressure, and the viscous compound thus obtained was dispersed with 20 mL of diethyl ether and kept at 0 °C overnight, which afforded the target compound as a crystalline precipitate. HRMS $[M - 1]^-$ calculated: 183.04. Found: 183.04. M.P. 160–162 °C. ^{1}H NMR (400 MHz, CD_3OD, 25 °C, TMS): δ (ppm) 2.50 (t, 2H, CH_2), 3.95 (t, 2H, CH_2), 5.60 (d, 1H, C5–H,), 7.65 (d, 1H, C6–H). ^{13}C NMR (125 MHz, DMSO-d_6, 25 °C, TMS): δ (ppm) 36.38, 46.45, 100.90, 147.63, 151.56, 165.65, 176.41. Anal. Calcd (found) for $C_7H_8N_2O_4$: C, 45.66 (45.57); H, 4.38 (4.33); N, 15.21 (15.14).

*Synthesis of [Cu(TAcO)$_2$(H$_2$O)$_4$]·4H$_2$O (**1**).* Copper(II) acetate monohydrate (0.100 g, 0.5 mmol) was added to a solution of thymine-1-acetic acid (0.184 g, 1 mmol) and potassium hydroxide (0.058 g, 1 mmol) in 10 mL of distilled water (pH = 5). The resulting mixture was refluxed and stirred for 3 h. Upon cooling, blue crystals appeared, which were filtered off; washed with water, ethanol, and ether; and dried in the air (0.112 g, 50% yield based on the metal). L-SIMS (ES^+ mode): $[L + Cu]^+$ = calculated, 246.65; found, 245.97. $[2L + Cu + H]^+$ = calculated, 431.15; found, 430.03. Anal. (%) Calcd (found) for $C_{14}H_{30}CuN_4O_{16}$: C, 29.29 (30.01); H, 5.23 (5.07); N, 9.76 (9.71). IR selected data (KBr, cm^{-1}): 3430(m), 1678(s), 1603(w), 1479(w), 1404(w), 1350(w), 1247(w), 869(w). ^{1}H NMR (400 MHz, D_2O, 25 °C, TMS, pH = 5.5): δ (ppm) 1.96 (d, 3H, CH_3), 3.57 (s, 2H, CH_2), 7.44 (s, 1H, C6–H). The purity of the crystal sample was checked by powder X-ray diffraction.

*Synthesis of [Cu(TAcO)$_2$(H$_2$O)$_2$]$_n$ (**2**).* A mixture of $CuCl_2·2H_2O$ (0.100 g, 0.58 mmol), thymine-1-acetic acid (0.216 g, 1.17 mmol), and potassium hydroxide (0.065 g, 1.17 mmol) was dissolved in 20 mL of distilled water and stirred for 3 h at 25 °C (pH = 2). The blue mixture obtained was filtered off. The blue solid obtained was washed with water, methanol, and ether and dried in the air (0.056 g, 21% yield based on the metal). The purity of the blue solid has been checked using powder X-ray diffraction. Blue crystals suitable for X-ray diffraction were obtained from the mother solution upon standing for 3 weeks at 25 °C. They were filtered off; washed with water, ethanol, and ether; and dried in the air (0.042 g, 15.5% yield based on the metal). Anal. (%) Calcd (found) for $C_{14}H_{18}CuN_4O_{10}$: C, 36.1 (36.2); H, 3.89 (3.89); N, 12.51 (12.39). IR selected data (KBr, cm^{-1}): 3165(m), 3038(m), 1672(s), 1562(s), 1426(m), 1408(m), 1353(w), 1254(w), 898(w).

*Synthesis of [Cu$_{1.5}$(TAcO)$_2$(H$_2$O)(OH)]$_n$·4H$_2$O (**3**).* The reaction was carried out as described above for compound **1** but at 25 °C instead. The blue suspension obtained was filtered off and the blue solution allowed to crystallize at 25 °C. After several days, blue crystals were formed, filtered, washed with water, and dried in the air (0.11 g, 34% yield based on the metal). Anal. (%) Calcd (found) for $C_{28}H_{42}Cu_3N_8O_{24}$: C, 31.56 (31.18); H, 3.94 (3.92); N, 10.52 (10.82). IR selected data (KBr, cm^{-1}): 3166(m), 3040(w), 1696(s), 1562(s), 1432(s), 1402(m), 1231(w), 901(w), 832(w), 763(w). The analysis of powder X-ray diffraction of the first solid isolated in this reaction is consistent with a mixture of compounds **1** and **3**.

*Synthesis of [Cu$_3$(UPrO)$_2$Cl$_2$(OH)$_2$(H$_2$O)$_2$]$_n$ (**4**).* UPrOH (0.050 g, 0.27 mmol.), $CuCl_2·2H_2O$ (0.070 g, 0.41 mmol), and distilled water (5 mL) were placed in a 10 mL Teflon liner stainless steel bomb and heated at 110 °C for 6 h under autogenous pressure. The reaction mixture was cooled down to ambient temperature, which afforded a light blue color clear solution. The solution was filtered and kept for slow evaporation. Blue crystals of complex **4** were obtained after several days (65 mg, 18% yield, based on HL precursor). HRMS (ES+ mode): $[L + Cu + H_2O]^+$ = calculated, 263.99; found, 264.03. $[2L+Cu+H]^+$ = calculated, 430.03; found, 430.02. (ES–) mode: $[3L+Cu]^-$ = calculated, 612.06 and 614.05; found, 612.04 and 614.04. Anal. (%) Calcd (found) for $C_{14}H_{20}Cl_2Cu_3N_4O_{12}$: C, 24.09 (23.76); H, 2.89 (3.10); N, 8.03 (7.83). IR selected data (KBr, cm^{-1}): 3412(w), 3034(w), 2832(m) 1682(s), 1436(s), 1361(s), 864(s).

RESULTS AND DISCUSSION

The reaction of thymine-1-acetic acid with copper(II) acetate or copper(II) chloride carried out at 25 °C and at different pH values led to the formation of one-dimensional coordination polymers (pH 2 for **2** and pH 5 for **3** and **4**). More energetic conditions, reflux or solvothermal, increase the yield of the mononuclear complex **1**. However, the reaction of uracile-1-propionic acid with copper(II) chloride under solvothermal conditions led selectively to compound **4**.

The IR spectra of the obtained compounds (**1**–**4**) show significant shifts in the C═O and C–O stretching vibrations relative to those found in the free ligands. Thus, in general upon copper coordination to the carboxylic groups the C–O vibrations undergoes a shift to lower frequencies, υ_{as}(C–O) of *ca.* 10–40 cm^{-1} and υ_{sim}(C–O) of *ca.* 40–100 cm^{-1}. This is in agreement with the coordination of the carboxylic groups from the ligands with copper(II) ions.

Structural Description. The crystal structure of compound **1** consists of discrete [Cu(TAcO-κO)$_2$(H$_2$O)$_4$] complexes and crystallization water molecules (Figure 2). The metal center (green polyhedra) presents a CuO_6 coordination environment with the usual Jahn–Teller tetragonally elongated octahedral

dx.doi.org/10.1021/ic401758w | *Inorg. Chem.* 2013, 52, 11428–11437

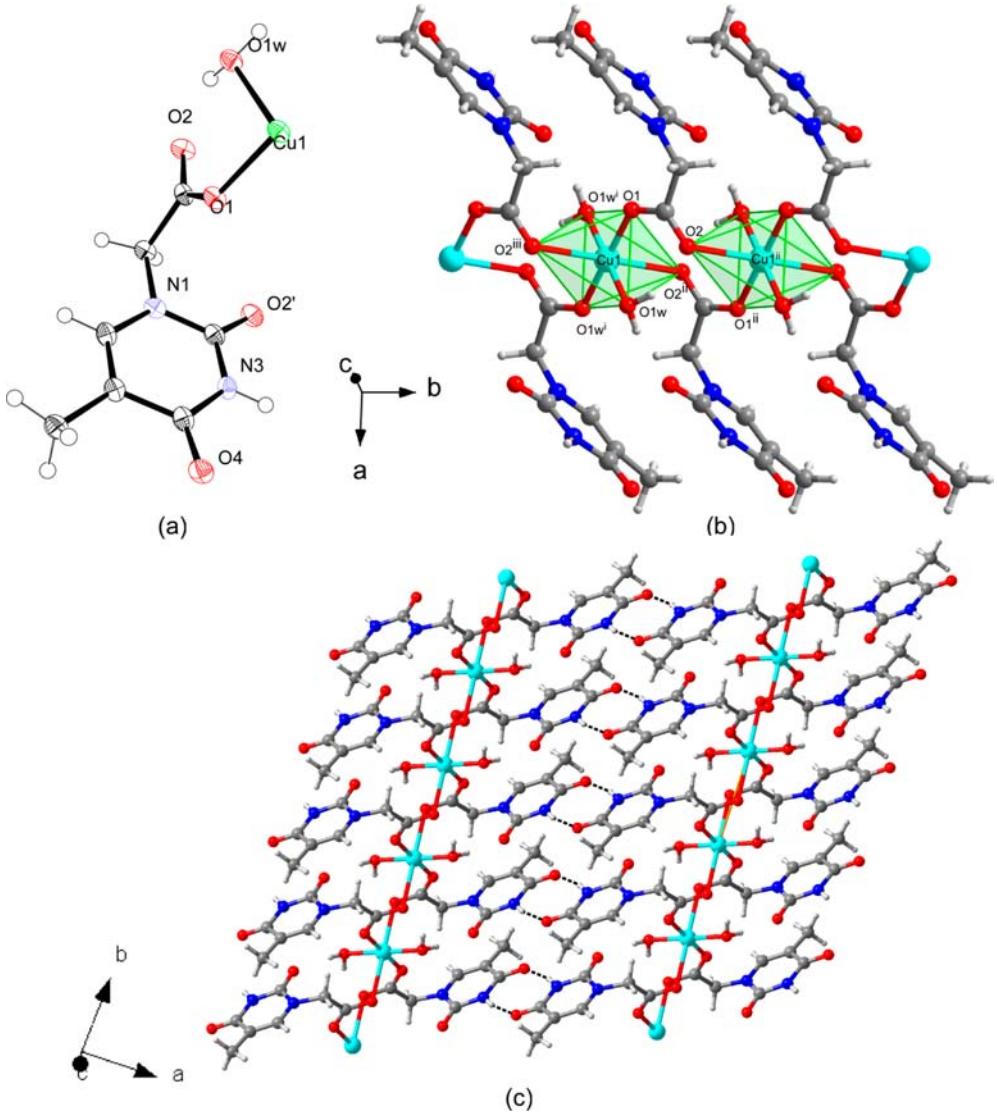

Figure 3. (a) ORTEP representation of the asymmetric unit of complex **2**. (b) Fragment of the polymeric chain of compound **2**. (c) T:T base pairing between adjacent polymeric chains to provide supramolecular sheets.

geometry (Table S2). The basal plane implies two carboxylate oxygen atoms from two TAcO ligands and two coordinated water molecules (O1w and O1w^{i}). The two apical positions are occupied by additional coordination water molecules (O2w and O2w^{i}) with longer coordination bond distances (2.5309(14) vs 1.9413(14) and 1.9595(13) Å). The functionalized thymine moiety coordinates only through one of its carboxylic oxygen atoms (Cu1−O1: 1.9595(13) Å), whereas the other is involved in an intramolecular hydrogen bonding interaction with the apical coordination water molecule. The thymine molecule not involved in metal coordination establishes an intricate network of hydrogen bonding interactions with the water molecules that provides cohesion to the 3D crystal building. There is no evidence of direct hydrogen bonding or aromatic interaction among the nucleobases.

Although compound **2** crystallizes under similar aqueous conditions, it presents a double bridged 1D polymeric complex in which the copper(II)/water ratio is lower, the TAcO ligand being forced to occupy the empty coordination sites of the elongated octahedral geometry (Figure 3). The carboxylato group of the thymine adopts a μ-1κO:2κO′ coordination mode in such a way that it is coordinated through O1 to the equatorial plane of one copper(II) atom and through O2 to the apical position of an adjacent metal center (1.945(2) and 2.624(2) Å, respectively). The carboxylate group is almost coplanar with the Cu1−O1 bond but almost perpendicular to Cu1^{ii}−O2. Two *trans* water molecules complete the coordination equatorial plane. These coordinated water molecules further contribute to the cohesion within the chain by means of intrachain hydrogen bonds that they establish as donors with the thymine O2′ and the carboxylate O2 oxygen atoms as acceptors. The copper···copper distance within the chain is 4.5896(3) Å. The thymine bases are projected outward from the 1D chain, allowing the establishment of complementary hydrogen bonding interactions (N3−H···O4, $d_{H\cdots O}$ = 1.99 Å) between thymine fragments belonging to adjacent chains. This interaction provides 2D supramolecular sheets of complex chains that are held together by means of weak van der Waals interactions (Figure 3c).

Compound **3** corresponds to a 1D polymeric complex in which hydroxide anions help the TAcO ligands to connect the copper(II) metal centers. In fact, two crystallographically

dx.doi.org/10.1021/ic401758w | *Inorg. Chem.* 2013, 52, 11428−11437

independent copper(II) centers are present in the crystal structure of this compound. Both are octahedrally coordinated, but Cu1, sited on a symmetry center, is bonded to two hydroxide anions and four oxygen atoms belonging to the carboxylate group of four TAcO ligands, whereas Cu2, located in a general position, completes its coordination polyhedron with two hydroxide anions, a water molecule, and three oxygen carboxylate atoms from three TAcO ligands. Both the hydroxide and the TAcO ligands act as bridges linking the metal centers within the chain. The hydroxide anion connects three metal centers in an almost symmetrical fashion (bond distances: 1.963−1.966 Å, Table S2). There are two crystallographically independent TAcO ligands that bridge adjacent metal centers showing different coordination modes. The first ligand, TAcO-1, uses its two carboxylate oxygen atoms to bridge three metal centers (μ_3-1κO:2κO:3$\kappa O'$), whereas the second ligand, TAcO-2, uses only one carboxylate oxygen atom to bridge two metal centers (μ-1κO:2κO) (Figure 4). The equatorial positions of the Cu coordination spheres are occupied by the carboxylato oxygen atoms of the TAcO-1 ligand, the hydroxide anion, and the water molecule with short coordination bond distances (1.93−1.99 Å). The TAcO-2 ligand and one carboxylato oxygen atom from the TAcO-1 ligand occupy the apical positions (2.34−2.68 Å). This connectivity scheme leads to a linear array of fused metal triangles that share an edge and the opposite vertex of each triangle where three different metal···metal distances could be identified (Cu1···Cu2, 3.003(2); Cu1···Cu2^{ii}, 3.302(2); and Cu2···Cu2^{ii}, 2.9734(14) Å). The thymine residue of the TAcO ligands remains, like in compounds **1** and **2**, free to establish additional supramolecular interactions that ensure the 3D cohesiveness of the crystal structure.

These supramolecular interactions comprise two different recognition processes involving thymine residues that hold chains together: (i) a double hydrogen bond (N23−H···O27, $d_{H\cdots O}$ = 2.01 Å) between the TAcO-2 ligands and (ii) two hydrogen bonds established between the TAcO-1 ligand and the coordinated water molecule and a carboxylate oxygen atom from another TAcO-1 ligand ($d_{H\cdots O}$ = 1.96 and 1.85 Å, respectively). The crystallization water molecules also reinforce previously described interactions by means of an extensive network of hydrogen bonds.

The structure of compound **4** consists of a $[Cu_3(UPrO)_2Cl_2(OH)_2(H_2O)_2]_n$ one-dimensional polymer running along the *a* axis. The asymmetric unit of complex **4** is composed of two crystallographically unique copper ions (Cu1 and Cu2) with Cu2 having half occupancy (Figure 5a). The nucleobase precursor behaves as a monoanionic ligand with both carboxylate oxygen atoms coordinated to the copper ions. The lattice is further neutralized by a μ_3-bridging hydroxo anion and a chloride anion (Figure 5a) along with a μ_2-bridging aqua ligand, also found in the lattice. As can be observed in Figure 5b, both copper centers show elongated octahedral geometries (due to the Jahn−Teller effect) with different coordination spheres. The Cu1 center is coordinated by one chloride and five oxygen atoms. The equatorial plane is formed by one oxygen atom from a carboxylate group (O1), two equivalent hydroxide anions (O4), and the chlorine anion (Cl1). The axial positions are occupied by a water molecule (O3) and a carboxylate oxygen atom (O2). The Cu−O equatorial bond lengths (1.951−1.988 Å) are much shorter than the axial ones (2.457−2.614 Å). The Cu2 ion lies on an inversion center and is coordinated by six oxygen atoms in a

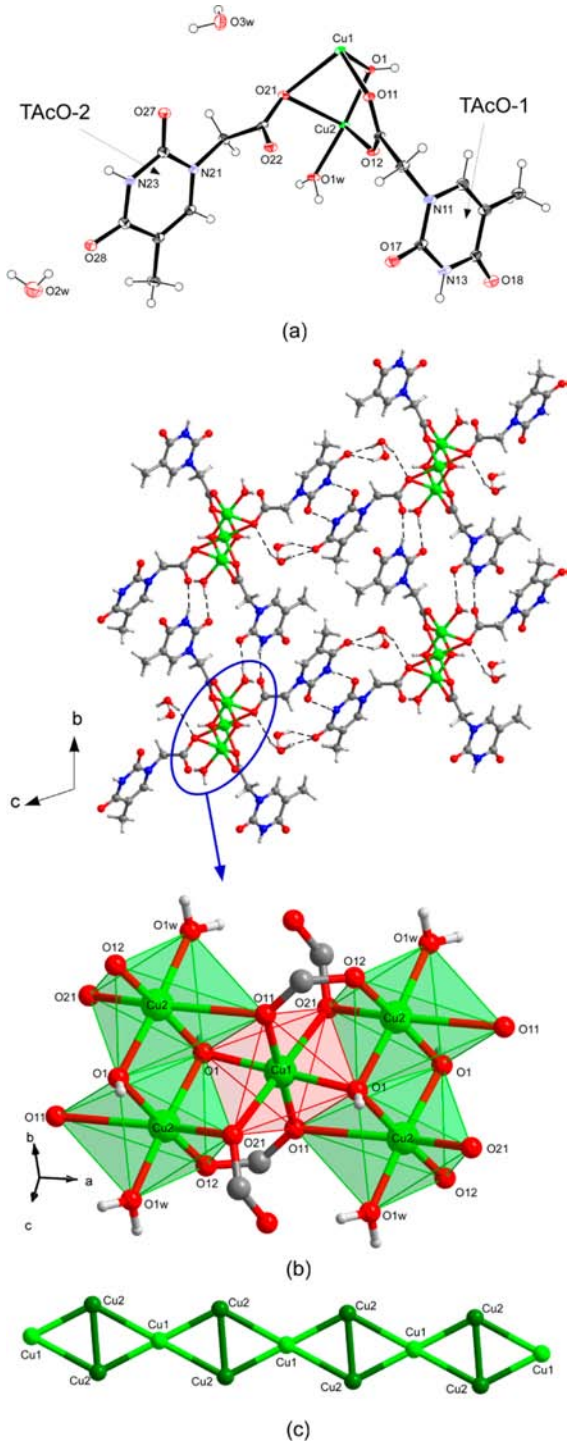

Figure 4. (a) ORTEP representation of the asymmetric unit of complex **3**. (b) Fragment of the polymeric chain and supramolecular structure of compound **3**. (c) Schematic representation of the chain topology. Crystallographically unique copper ions are highlighted with different colors.

Jahn−Teller elongated octahedral geometry. The equatorial plane is formed by two oxygen atoms from two carboxylate groups (O2 and O2*, with Cu2−O2 = 1.959(3) Å) and two equivalent μ_3-bridging hydroxide anions (O4 and O4*, with Cu2−O4 = 1.957(3) Å). The axial positions are occupied by two water molecules (O3 and O3* with a much longer bond length of 2.427(4) Å). All the Cu−O and Cu−Cl bond lengths

dx.doi.org/10.1021/ic401758w | *Inorg. Chem.* 2013, 52, 11428−11437

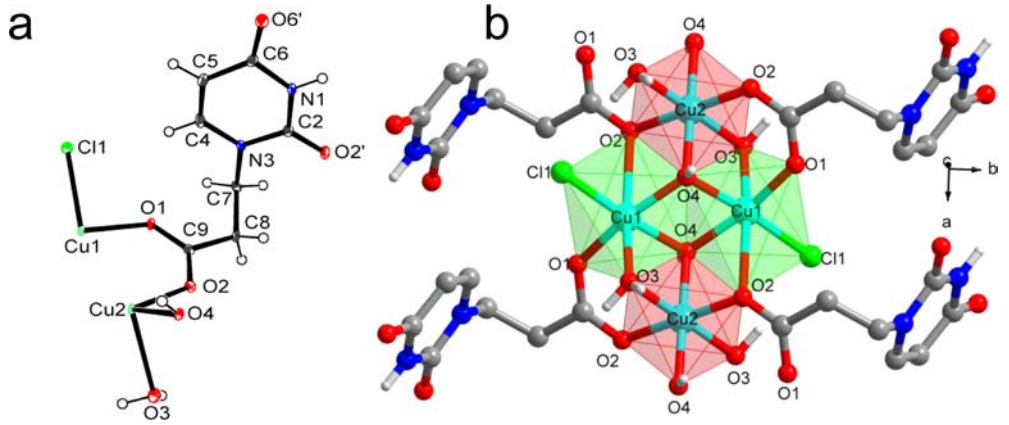

Figure 5. (a) ORTEP representation of complex **4** at 35% probability level. (b) Part of the lattice of **4** with coordination atmosphere around Cu centers.

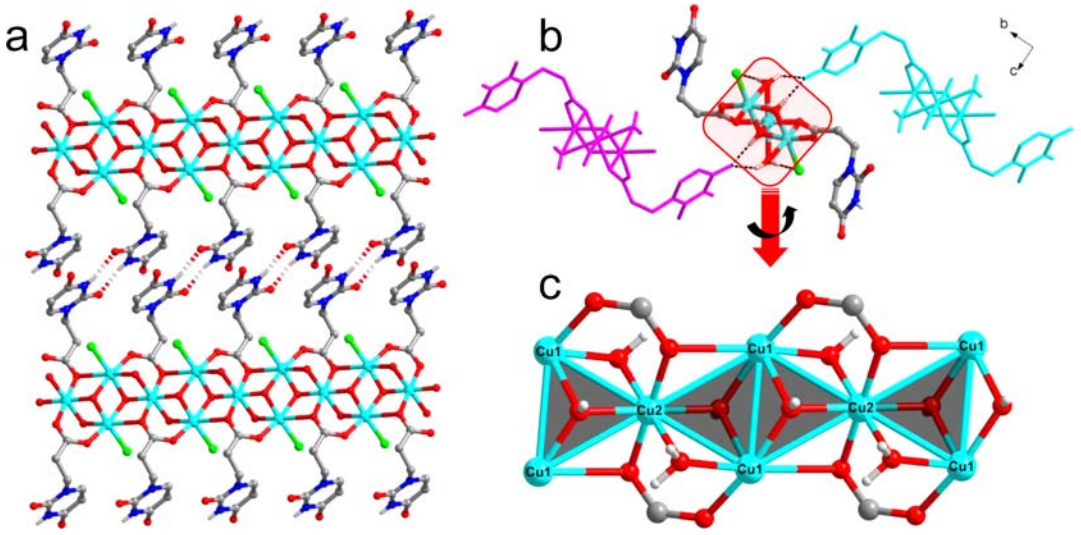

Figure 6. (a) U:U base pairing in the crystal lattice as shown with fragmented bonds (view close to *c* axis). (b) Involvement of hydroxo and aqua ligands in the H-bonding. (c) Schematic representation of the chain topology of complex **4**.

are in the typical range observed in other Cu(II) octahedral complexes.[45]

It is interesting to note that both oxygen atoms of the carboxylate group (O1 and O2) interact with the copper centers in a different manner. O1 acts as monodentate toward Cu1, whereas O2 bridges Cu1 and Cu2 centers, giving rise to an overall tridentate (μ_3-1κO:2κO:3$\kappa O'$) coordination mode for the carboxylate group. All the copper atoms are bridged by μ_3-OH, μ_2-aqua, and μ_3-carboxylate ligands to generate a ribbon-like extended Cu−O network where all the interconnected copper atoms lie on the same plane. As observed in compound **3**, the connectivity array consists of fused metal triangles that share an edge and the opposite vertex of each triangle where three different metal···metal distances can be found (Cu1···Cu2 = 2.962(2) Å, Cu1···Cu2^{i} = 3.220(2) Å, and Cu1···Cu1^{iii} = 3.099(2) Å, Figure 6c).

Further reinforcement to the lattice comes from the hydrogen bonding interaction. The uracil nucleobases are positioned on each side of the chain structure and involved in the well-known U:U base pairing scheme by exploiting N−H···O hydrogen bonding ($d_{H\cdots O}$ = 1.988 Å) with the uracil moiety present in the adjacent chain as shown in Figure 6a. This interaction extends the lattice along the *b* axis. The hydroxo and aqua ligands are also involved in H-bonding interactions acting as H-donors for the remaining exocylic oxygen atom (O6′) of the uracil moiety (Table S3 for H bonding) as shown in Figure 6b. These H-interactions further extend the lattice along the *c* axis, increasing the dimensionality of the crystal structure.

Magnetic Properties. Compound **2** presents a magnetic behavior typical of almost isolated copper(II) metal centers; the $\chi_m T$ curve remains constant upon cooling (0.425 cm^3 K mol^{-1}) and, only at temperatures below 15 K, decreases slightly (0.410 cm^3 K mol^{-1} at 5 K; Figure S1). Considering the structural features, the experimental data were least-square fitted with a numerical expression proposed for an antiferromagnetic copper(II) uniform chain[46] that leads to *J* (triplet-singlet gap) = −0.2 cm^{-1}, *g* = 2.14, and *R* = 1.7 × 10^{-6}, *R* being the agreement factor defined as $\sum_i[(\chi_M T)_{obs}(i) - (\chi_M T)_{calc}(i)]^2/\Sigma_i[(\chi_M T)_{obs}(i)]^2$. This almost negligible antiferromagnetic coupling can be understood in terms of the nature of the orbital involved in the superexchange interactions, together with the arrangement of the bridging ligand. The unpaired electron of the copper(II) ion is essentially described by a magnetic orbital built from the $d_{x^2-y^2}$ metallic orbital and located mainly in the basal plane. The carboxylato, with a basal (short, 1.945(2) Å)−axial (long, 2.624(2) Å) bridging mode

dx.doi.org/10.1021/ic401758w | *Inorg. Chem.* 2013, 52, 11428−11437

leads to an almost nil overlap between the two metal-centered magnetic orbitals, resulting in a weak anti- or ferromagnetic (when the overlap is zero, accidental orthogonality) coupling.[47,48]

Variable temperature susceptibility measurements of compounds **3** and **4** (Figure 7) reveal, despite their structural

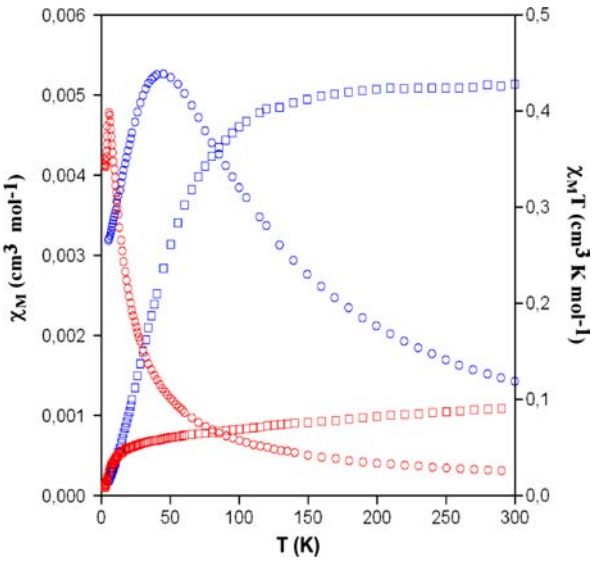

Figure 7. Temperature variable $\chi_m T$ (squares) and χ_m (circles) curves per copper(II) atom for compounds **3** (blue) and **4** (red).

similarity, a different magnetic behavior. The $\chi_m T$ value per copper(II) atom for compound **3** at room temperature is 0.430 cm^3 K mol^{-1}. This value remains almost constant until 120 K and shows a sharp decrease upon cooling to reach a value of 0.012 cm^3 K mol^{-1} at 2 K. The thermal evolution of the magnetic susceptibility shows the presence of a rounded maximum around 43 K. This behavior is indicative of dominant moderate antiferromagnetic interactions between the Cu(II) atoms. Compound **4** presents a $\chi_m T$ value at room temperature of 0.092 cm^3 K mol^{-1} which is well below the expected value for a copper(II) metal center. This value slowly decreases upon cooling down to 15 K, and then it drops to a value of 0.009 cm^3 K mol^{-1} at 2 K. The magnetic susceptibility curve shows a sharp maximum at 5 K. The low $\chi_m T$ value at room temperature and its slow decrease upon cooling suggests the presence of very strong antiferromagnetic coupling between some but not all the copper(II) centers. In fact, from the maximum in the χ_m curve at 5 K it can be inferred that the remaining copper(II) atoms present only weak antiferromagnetic interactions.

Figure 8 depicts the different superexchange coupling constants taking place in compounds **3** and **4** that should be taken into account in order to model their magnetic behavior. As far as we know, no available mathematical expression could account for the scheme of magnetic interactions taking place within the polymeric chains of these compounds. Therefore, we have estimated the individual J magnetic coupling constant for each magnetic superexchange pathway (J_1, J_2, J_3) from quantum computational calculations performed over simplified fragments of the polymeric chains. The magnetic exchange interaction between the open-shell electrons of a magnetic system within the DFT methods[49−51] is based on spin-polarized or unrestricted DFT calculations, in combination with the broken

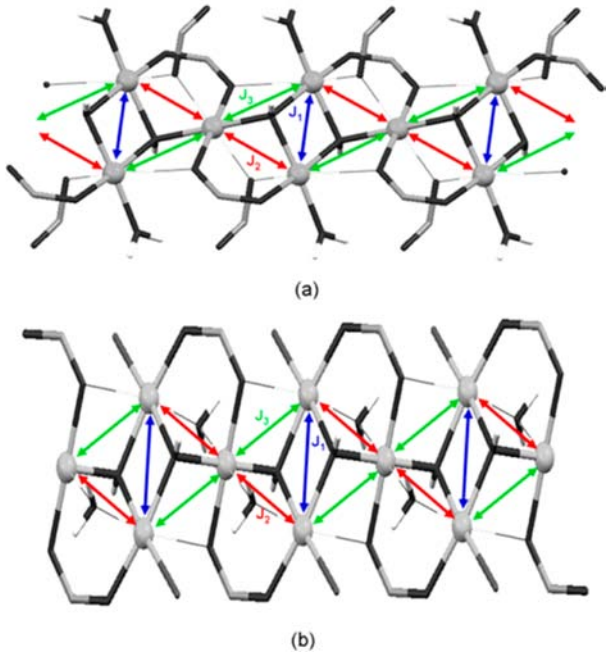

Figure 8. Magnetic superexchange pathways in compounds **3** (a) and **4** (b). Thinner bonds represent the elongated coordination bonds due to the Jahn−Teller effect of the copper(II) metal centers. Only the carboxylate groups of the thymine (a) and uracile (b) modified ligands are represented for clarity.

symmetry (BS) approach.[52−57] This approach has proven to be a powerful tool in the prediction and interpretation of magnetic properties of a large variety of magnetic systems, as well as for revealing and tracing magneto-structural correlations.[58] The broken symmetry treatment results in a solution that is an eigenstate of S_z (with eigenvalue S_{min}) but not of S_2, which can be written as a weighted average of the energies of the pure spin multiplets. In order to analyze the results, the approximate projection method introduced by Yamaguchi and co-workers to account for the spin contamination was employed in the approximate spin projected scheme.[53,59,60] The hybrid B3LYP method,[61] as implemented in Gaussian 03, was used in all calculations.[62] The exact Hartree−Fock-type exchange was mixed with Becke's expression for the exchange functional,[61] and the Lang−Yong−Parr correlation functional[63] was used. The Gaussian implemented 6-31G(d) basis set has been employed throughout this work. In order to reproduce as close as possible the chemical surrounding for the computed superexchange coupling for every adjacent pair of metal centers, the additional metal centers coordinated to the bridging ligands were replaced by zinc(II) atoms without any further change in the coordination bond distances. The coordination sphere of every metal center is completed by the original ligand molecules/anions except for uracil-propionate that was replaced by acetate anions. The results are summarized in Table 1. Figures of the models and the spin density distribution for the triplet and singlet states are provided as Supporting Information (Figure S2).

The results indicate that the most notorious difference takes place for the double hydroxide bridge mediated superexchange interaction (J_1) that should be weakly ferromagnetic (J_1 = +28 cm^{-1}) for compound **3** according to the computational simulation but strongly antiferromagnetic ($J_1 \approx -300$ cm^{-1}) for compound **4**. The calculated spin-density distribution for

dx.doi.org/10.1021/ic401758w | Inorg. Chem. 2013, 52, 11428−11437

Table 1. Magnetically Relevant Structural Parameters and Computed Magnetic Coupling Constants for Compounds 3 and 4[a]

			Compound **3**			
Cu2···Cu2	Cu2−O−Cu2	Cu_2O_2 planarity[b]		H−O···O	Cu2−O	J_1
2.97 Å	98.3°	0.0°		53.5°	1.97 Å	+28 cm^{-1}
Cu1···Cu2	Cu1−O−Cu2	$Cu1-O_{OCO}$	$Cu2-O_{OCO}$	$Cu1-O_{OH}$	$Cu2-O_{OH}$	J_2
3.00 Å	99.7°	1.99 Å	1.93 Å	1.96 Å	1.97 Å	+36 cm^{-1}
Cu1···Cu2	Cu1−O−Cu2	$Cu1-O_{OH}$		$Cu2-O_{OH}$		J_3
3.30 Å	114.4°	1.96 Å		1.97 Å		−8 cm^{-1}
			Compound **4**			
Cu1···Cu1	Cu2−O−Cu2	Cu_2O_2 planarity		H−O···O	Cu1−O	J_1
3.10 Å	103.6°	0.0°		44.7°	1.96/1.99 Å	−295 cm^{-1}
Cu1···Cu2	Cu1−O−Cu2	$Cu1-O_{OCO}$	$Cu2-O_{OCO}$	$Cu1-O_{OH}$	$Cu2-O_{OH}$	J_2
2.96 Å	97.3°	1.95 Å	1.96 Å	1.99 Å	1.96 Å	−18 cm^{-1}
Cu1···Cu2	Cu1−O−Cu2	$Cu1-O_{OH}$		$Cu2-O_{OH}$		J_3
3.22 Å	110.7°	1.96 Å		1.96 Å		−27 cm^{-1}

[a]The spin Hamiltonian is defined by $\hat{H} = -J\sum\hat{S}_i\cdot\hat{S}_{i+1}$. [b]$Cu_2O_2$ planarity defined as the dihedral angle between the two OCuO planes in the Cu_2O_2 central core.

the ground state ($S = 0$) is shown in Figure 9. These results are in good agreement with previous experimental results that show

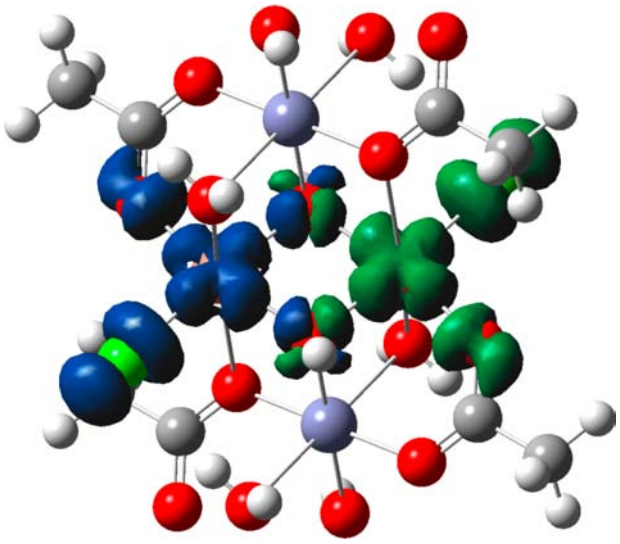

Figure 9. Calculated spin-density distribution of the ground state ($S = 0$) of compound **4** with a threshold level of 0.0015. The blue spheres correspond to Zn(II) atoms.

the superexchange coupling constants mediated by hydroxide ligands range from −700 to +300 cm^{-1}.[64−66] For di-μ-hydroxido-bridged Cu(II) binuclear complexes, the classical magneto-structural correlation between the Cu−O−Cu bond angle (φ) and the experimental superexchange constant (J) ($J = -74.538\varphi + 7270$ cm^{-1}) indicates that those complexes are antiferromagnetic for $\varphi > 98°$ but ferromagnetic for smaller angles.[67] However, more recently advanced theoretical calculations using different density functional methods have demonstrated that other structural parameters such as small variances in the Cu−O(bridge) distances, the out of plane displacement of the hydroxo hydrogen atom, the nonplanarity of the Cu_2O_2 core, and the distance from copper atom to the basal plane can play an important role on the fine-tuning of the superexchange coupling.[68,69]

In fact, a perusal of the CSD database allows us to locate the compounds with structural parameters around the double hydroxido magnetic superexchange pathway closer to compounds **3** and **4**. For compound **3**, the most similar magnetically characterized compound corresponds to a 1D polymeric compound, $[Cu_3(\mu\text{-adipato})_2(\mu_3\text{-OH})_2(\mu\text{-H}_2O)_4]_n$ (Cu−O−Cu, 98.5°; Cu_2O_2 planarity, 0.0°; H−O···O, 47.3°; Cu−O, 1.97 Å) for which a J value of −54.5 cm^{-1} is reported.[70] The nature of the magnetic interaction in this example is the opposite of the ferromagnetic behavior estimated from DFT calculations, but the energy difference lies inside the accuracy for this kind of calculation. On the other hand, the ferromagnetic interaction predicted in compound **3** for the second superexchange pathway (J_2) is explained by means of the orbital counter-complementarity between the μ-carboxylato-κO:κO′ bridge and the hydroxide bridge with $\varphi > 98°$.[71] For φ angles below this threshold, the μ-hydroxido induced SOMO energy difference is so small in comparison to that generated by the carboxylato ligand that the antiferromagnetism dominates this superexchange pathway as computed for compound **4**.

The Cu_2O_2 central core with closer structural resemblance to that of compound **4** corresponds to a dinuclear compound $[LCu^{II}(\mu\text{-OH})_2Cu^{II}L](BF_4)_2$ [L = tris(3-isopropyl-4,5-trimethylenepyrazolyl)methane] (Cu−O−Cu, 103.3 and 104.1°; Cu_2O_2 planarity, 2.7°; H−O···O, 56.3 and 53.1°; Cu···Cu, 3.06 Å; Cu−O, 1.93−1.95 Å) where a J value of −633 cm^{-1} has been found.[72] This last example reinforces the hypothesis of the presence of very strong antiferromagnetic interactions between the metal centers bridged by the double hydroxido bridge in compound **4**. Therefore, the $\chi_m T$ value at 300 K would correspond only to the weakly antiferromagnetically coupled copper(II) metal center, which is not coordinated to this hydroxido double bridge (just one-third of the total metal centers).

Electrical Conductivity Studies. Two probe direct current (dc) electrical conductivity measurements at 300 K were performed in six single crystals of compound **2**, four of compound **3**, and in two pressed pellets of compound **4** (due to the impossibility to obtain suitable crystals for these measurements). The conductivity values at 300 K were obtained applying voltages from +10 to −10 V. For complexes **2**−**4**, the room temperature dc conductivity values are 1.0×10^{-9}, 6.8×10^{-6}, and 7.7×10^{-8} S·cm^{-1}, respectively, suggesting a semiconductor behavior in all cases. For compounds **2** and **3**, we have also performed dc electrical measurements with the four contacts method in the temperature range 300−400 K in

dx.doi.org/10.1021/ic401758w | Inorg. Chem. 2013, 52, 11428−11437

order to confirm the semiconducting behavior and determine the activation energy. These measurements show activation energies of *ca.* 1.3 eV for both complexes (Figures S4 and S5). As expected, at 400 K the conductivity is higher with values of 1×10^{-6} and 5×10^{-7} S cm^{-1} in complexes **2** and **3**, respectively. Note that the crystals used for the conductivity measurements at high temperatures present some microfractures after the thermal cycles under a vacuum, indicative of a degradation of the quality of the single crystals that justify the fact that in compound **3** the conductivity in the cooling scan is lower than in the heating scan (Figure S4) and also that the conductivity at 400 K in some crystals is lower than at 300 K in other crystals. Note also that the conductivity of compound **4** should be higher than the reported value since the measurements in pressed pellets usually yield conductivity values two or more orders of magnitude lower than the corresponding measurements on single crystals.[18]

CONCLUSIONS

The direct reactions between the two building blocks, Cu(II) metal ions and modified nucleobases (thymine-1-acetic acid and the uracil-1-propionic acid), have allowed the isolation of three unprecedented one-dimensional coordination polymers. The chain structure of compound **2** shows a weak antiferromagnetic interaction between the Cu(II) centers, while **3** and **4** show very different magnetic properties, despite presenting a very similar chain structure. Moderate-weak antiferromagnetic interactions have been found between Cu(II) atoms in complex **3**, whereas a combination of strong and weak antiferromagnetic interactions has been found in complex **4**. Additionally, compounds **2**−**4** behave as semiconductors and constitute rare examples of polymeric magnetic semiconductors.

These physical properties and chain structures of these polymers showing their H-bonding donor and acceptor sites potentially available for supramolecular interactions with suitable molecules, suggest potential application of these coordination polymers for the construction of functional complex structures by supramolecular interaction with specific DNA or oligonucleotide sequences. Work in this direction is currently in progress.

ASSOCIATED CONTENT

Supporting Information

X-ray crystallographic files in CIF format for compounds **1**−**4** (CCDC 949549−949552). Crystallographic data, selected bond lengths and angles, hydrogen bonding interactions, temperature variable $\chi_m T$ and χ_m curves, calculated coupling constants, and thermal variation of the dc conductivity for compounds **1**−**4**. This material is available free of charge via Internet at http://pubs.acs.org.

AUTHOR INFORMATION

Corresponding Authors

*E-mail: pilar.amo@uam.es.
*E-mail: felix.zamora@uam.es.

Notes

The authors declare no competing financial interest.

ACKNOWLEDGMENTS

We thank financial support from the Spanish Ministerio de Economía y Competitividad (MAT2010-20843-C02-01, MAT2008-05690/MAT, CTQ-2011-26507, FIS2009-12721, and ACI2009-0969), Comunidad de Madrid (project S-0505/MAT/0303), Gobierno Vasco (IT-280-07), Generalitat Valenciana (Projects Prometeo 2009/95 and ISIC), and EU (FP6-029192). Work in India is supported by DAE-SRC Outstanding Investigator Award and DST J. C. Bose National Fellowship to S.V.

REFERENCES

(1) Pinheiro, A. V.; Han, D.; Shih, W. M.; Yan, H. *Nat. Nanotechnol.* **2011**, *6*, 763−772.
(2) Burley, G. A.; Gierlich, J.; Mofid, M. R.; Nir, H.; Tal, S.; Eichen, Y.; Carell, T. *J. Am. Chem. Soc.* **2006**, *128*, 1398−1399.
(3) Nguyen, K.; Monteverde, M.; Filoramo, A.; Goux-Capes, L.; Lyonnais, S.; Jegou, P.; Viel, P.; Goffman, M.; Bourgoin, J.-P. *Adv. Mater.* **2008**, *20*, 1099−1104.
(4) Nishinaka, T.; Takano, A.; Doi, Y.; Hashimoto, M.; Nakamura, A.; Matsushita, Y.; Kumaki, J.; Yashima, E. *J. Am. Chem. Soc.* **2005**, *127*, 8120−8125.
(5) Dong, L.; Hollis, T.; Fishwick, S.; Connolly, B. A.; Wright, N. G.; Horrocks, B. R.; Houlton, A. *Chem.—Eur. J.* **2007**, *13*, 822−828.
(6) Batten, S. R.; Neville, S. M.; Turner, D. *Coordination Polymers: Design, Analysis and Applications*; RSC Publishing: London, 2009; Vol. *7*.
(7) Stock, N.; Biswas, S. *Chem. Rev.* **2012**, *112*, 933−969.
(8) O'Keeffe, M.; Yaghi, O. M. *Chem. Rev.* **2012**, *112*, 675−702.
(9) Janiak, C. *Dalton Trans.* **2003**, 2781−2804.
(10) Gu, Z. Y.; Yang, C. X.; Chang, N.; Yan, X. P. *Acc. Chem. Res.* **2012**, *45*, 734−745.
(11) Wu, H. H.; Gong, Q. H.; Olson, D. H.; Li, J. *Chem. Rev.* **2012**, *112*, 836−868.
(12) Han, S. S.; Mendoza-Cortes, J. L.; Goddard, W. A. *Chem. Soc. Rev.* **2009**, *38*, 1460−1476.
(13) Uemura, T.; Yanai, N.; Kitagawa, S. *Chem. Soc. Rev.* **2009**, *38*, 1228−1236.
(14) Spokoyny, A. M.; Kim, D.; Sumrein, A.; Mirkin, C. A. *Chem. Soc. Rev.* **2009**, *38*, 1218−1227.
(15) Cui, Y. J.; Yue, Y. F.; Qian, G. D.; Chen, B. L. *Chem. Rev.* **2012**, *112*, 1126−1162.
(16) Wang, C.; Zhang, T.; Lin, W. B. *Chem. Rev.* **2012**, *112*, 1084.
(17) Kurmoo, M. *Chem. Soc. Rev.* **2009**, *38*, 1353−1379.
(18) Givaja, G.; Amo-Ochoa, P.; Gomez-Garcia, C. J.; Zamora, F. *Chem. Soc. Rev.* **2012**, *41*, 115−147.
(19) Welte, L.; Calzolari, A.; di Felice, R.; Zamora, F.; Gómez-Herrero, J. *Nat. Nanotechnol.* **2010**, *5*, 110−115.
(20) Hermosa, C.; Álvarez, J. V.; Azani, M. R.; Gómez-García, C. J.; Fritz, M.; Soler, J. M.; Gómez-Herrero, J.; Gómez-Navarro, C.; Zamora, F. *Nat. Commun.* **2013**, *4*, 1709.
(21) (a) Gomez-Herrero, J.; Zamora, F. *Adv. Mater.* **2011**, *23*, 5311−5317. (b) Welte, L.; García-Couceiro, U.; Castillo, O.; Olea, D.; Polop, C.; Guijarro, A.; Luque, A.; Gómez-Rodríguez, J. M.; Gómez-Herrero, J.; Zamora, F. *Adv. Mater.* **2009**, *21*, 2025−2028.
(22) Srivatsan, S. G.; Parvez, M.; Verma, S. *Chem.—Eur. J.* **2002**, *8*, 5184−5191.
(23) Mishra, A. K.; Purohit, C. S.; Kumar, J.; Verma, S. *Inorg. Chim. Acta* **2009**, *362*, 855−860.
(24) Lehn, J. M. *Science* **2002**, *295*, 2400−2403.
(25) Yang, E.-C.; Chan, Y.-N.; Liu, H.; Wang, Z.-C.; Zhao, X.-J. *Cryst. Growth. Des.* **2009**, *9*, 4933−4944.
(26) Sanz Miguel, P. J.; Amo-Ochoa, P.; Castillo, O.; Houlton, A.; Zamora, F. *Supramolecular Chemistry of Metal-Nucleobase Complexes*; Wiley-VCH: Chichester, U.K., 2009.
(27) Srivatsan, S. G.; Parvez, M.; Verma, S. *J. Inorg. Biochem.* **2003**, *97*, 340−344.
(28) Rother, I. B.; Freisinger, E.; Erxleben, A.; Lippert, B. *Inorg. Chim. Acta* **2000**, *300*, 339−352.
(29) Sheldrick, W. S. *Acta Crystallogr., Sect. B* **1981**, *37*, 945−946.

(30) García-Terán, J. P.; Castillo, O.; Luque, A.; García-Couceiro, U.; Román, P.; Lezama, L. *Inorg. Chem.* **2004**, *43*, 4549−4551.
(31) Pérez-Yáñez, S.; Castillo, O.; Cepeda, J.; García-Terán, J. P.; Luque, A.; Román, P. *Inorg. Chim. Acta* **2011**, *365*, 211−219.
(32) Perez-Yanez, S.; Beobide, G.; Castillo, O.; Cepeda, J.; Luque, A.; Roman, P. *Cryst. Growth. Des.* **2012**, *12*, 3324−3334.
(33) Purohit, C. S.; Verma, S. *J. Am. Chem. Soc.* **2006**, *128*, 400−401.
(34) Purohit, C. S.; Mishra, A. K.; Verma, S. *Inorg. Chem.* **2007**, *46*, 8493−8495.
(35) Kruger, T.; Ruffer, T.; Lang, H.; Wagner, C.; Steinborn, D. *Inorg. Chem.* **2008**, *47*, 1190−1195.
(36) Yang, E.-C.; Zhao, H.-K.; Feng, Y.; Zhao, X.-J. *Inorg. Chem.* **2009**, *48*, 3511−3513.
(37) Amo-Ochoa, P.; Alexandre, S. S.; Hribesh, S.; Galindo, M. A.; Castillo, O.; Gómez-García, C. J.; Pike, A. R.; Soler, J. M.; Houlton, A.; Zamora, F. *Inorg. Chem.* **2013**, *52*, 5290−5299.
(38) Xue, W.; Wang, B.-Y.; Zhu, J.; Zhang, W.-X.; Zhang, Y.-B.; Zhao, H.-X.; Chen, X.-M. *Chem. Commun.* **2011**, *47*, 10233−10235.
(39) Olea, D.; Alexandre, S. S.; Amo-Ochoa, P.; Guijarro, A.; de Jesus, F.; Soler, J. M.; de Pablo, P. J.; Zamora, F.; Gomez-Herrero, J. *Adv. Mater.* **2005**, *17*, 1761−1765.
(40) Amo-Ochoa, P.; Castillo, O.; Alexandre, S. S.; Welte, L.; de Pablo, P. J.; Rodriguez-Tapiador, M. I.; Gomez-Herrero, J.; Zamora, F. *Inorg. Chem.* **2009**, *48*, 7931−7936.
(41) Earnshaw, A. *Introduction to Magnetochemistry*; Academy Press: London, 1968.
(42) Ma, J.-F.; Liu, J.-F.; Xing, Y.; Jia, H.-Q.; Lin, Y.-H. *J. Chem. Soc., Dalton Trans.* **2000**, *0*, 2403−2407.
(43) Biradha, K.; Fujita, M. *J. Chem. Soc., Dalton Trans.* **2000**, *0*, 3805−3810.
(44) Richardson, C.; Steel, P. J.; D'Alessandro, D. M.; Junk, P. C.; Keene, F. R. *Dalton Trans.* **2002**, *0*, 2775−2785.
(45) Meng, W.-L.; Liu, G.-X.; Okamura, T.-A.; Kawaguchi, H.; Zhang, Z.-H.; Sun, W.-Y.; Ueyama, N. *Cryst. Growth. Des.* **2006**, *6*, 2092−2101.
(46) Bonner, J. C.; Fisher, M. E. *Phys. Rev.* **1964**, *135*, 640−658.
(47) Wen, D.-C.; Liu, S.-X.; Ribas, J. *Inorg. Chem. Commun.* **2007**, *10*, 661−665.
(48) Han, Z.; Zhao, Y.; Peng, J.; Gómez-García, C. J. *Inorg. Chem.* **2007**, *46*, 5453−5455.
(49) Parr, R. G.; Yang, W. *Density-Functional Theory of Atoms and Molecules*; Oxford University Press: New York, 1989.
(50) Hohenberg, P.; Kohn, W. *Phys. Rev.* **1964**, *136*, B864.
(51) Kohn, W.; Sham, L. J. *Phys. Rev.* **1965**, *A140*, 1133.
(52) Daul, C. I.; Bencini, A. *Reviews of Modern Quantum Chemistry, Part II*; World Scientific: Singapore, 2002.
(53) Nagao, H.; Nishino, M.; Shigeta, Y.; Soda, T.; Kitagawa, Y.; Onishi, T.; Yoshioka, Y.; Yamaguchi, K. *Coord. Chem. Rev.* **2000**, *198*, 265−295.
(54) Noodleman, L.; Peng, C. Y.; Case, D. A.; Mouesca, J. M. *Coord. Chem. Rev.* **1995**, *144*, 199−244.
(55) Noodleman, L. *J. Chem. Phys.* **1981**, *74*, 5737−5743.
(56) Noodleman, L.; Norman, J. G. *J. Chem. Phys.* **1979**, *70*, 4903−4911.
(57) Bencini, A.; Totti, F. *Int. J. Quantum Chem.* **2005**, *101*, 819−825.
(58) Ruiz, E. *Principles and Applications of Density in Inorganic Chemistry II*; Springer: Berlin, 2004; Book Series: Structure and Bonding, Vol. *113*, p 71.
(59) Mitani, M.; M., H.; Takano, Y.; Yamaki, D.; Yoshioka, Y.; Yamaguchi, K. *J. Chem. Phys.* **2000**, *113*, 4035−4041.
(60) Onishi, T.; Takano, Y.; Kitagawa, Y.; Kawakami, T.; Yoshioka, Y.; Yamaguchi, K. *Polyhedron* **2001**, *20*, 1177−1184.
(61) Becke, A. D. *J. Chem. Phys.* **1993**, *98*, 5648−5652.
(62) Frisch, M. J.; Trucks, G. W.; Schlegel, H. B.; Scuseria, G. E.; Robb, M. A.; Cheeseman, J. R.; Scalmani, G.; Barone, V.; Mennucci, B.; Petersson, G. A.; Nakatsuji, H.; Caricato, M.; Li, X.; Hratchian, H. P.; Izmaylov, A. F.; Bloino, J.; Zheng, G.; Sonnenberg, J. L.; Hada, M.; Ehara, M.; Toyota, K.; Fukuda, R.; Hasegawa, J.; Ishida, M.; Nakajima, T.; Honda, Y.; Kitao, O.; Nakai, H.; Vreven, T.; Montgomery, J. A., Jr.; Peralta, J. E.; Ogliaro, F.; Bearpark, M.; Heyd, J. J.; Brothers, E.; Kudin, K. N.; Staroverov, V. N.; Kobayashi, R.; Normand, J.; Raghavachari, K.; Rendell, A.; Burant, J. C.; Iyengar, S. S.; Tomasi, J.; Cossi, M.; Rega, N.; Millam, N. J.; Klene, M.; Knox, J. E.; Cross, J. B.; Bakken, V.; Adamo, C.; Jaramillo, J.; Gomperts, R.; Stratmann, R. E.; Yazyev, O.; Austin, A. J.; Cammi, R.; Pomelli, C.; Ochterski, J. W.; Martin, R. L.; Morokuma, K.; Zakrzewski, V. G.; Voth, G. A.; Salvador, P.; Dannenberg, J. J.; Dapprich, S.; Daniels, A. D.; Farkas, Ö.; Foresman, J. B.; Ortiz, J. V.; Cioslowski, J.; Fox, D. J. *Gaussian 09*, Revision A.1; Gaussian, Inc.: Wallingford, CT, 2009.
(63) Lee, C.; Yang, W.; Parr, R. G. *Phys. Rev.* **1988**, *37*, 785−789.
(64) Miller, J. S.; Drillon. M. *Magnetism: Molecules to Materials*; Wiley-VCH: Weinheim, Germany, 2001−2005; Vols. *1*−*5*.
(65) Coronado, E.; Delhaes, P.; Gatteschi, D.; Miller, J. S. *Nato ASI Series*; Kluwer: Dordrecht, The Netherlands, 1996; Vol. *321*.
(66) Kahn, O. *Molecular Magnetism*; VCH Publishers: New York, 1993.
(67) Crawford, V. H.; Richardson, H. W.; Wasson, J. R.; Hodgson, D. J.; Hatfield, W. E. *Inorg. Chem.* **1976**, *15*, 2107−2110.
(68) Ruiz, E.; Alemany, P.; Alvarez, S.; Cano, J. *J. Am. Chem. Soc.* **1997**, *119*, 1297−1303.
(69) Ruiz, E.; Alvarez, S. *Chem. Commun.* **1998**, *0*, 2767−2768.
(70) Bakalbassis, E. G.; Korabik, M.; Michailides, A.; Mrozinski, J.; Raptopoulou, C.; Skoulika, S.; Terzis, A.; Tsaousis, D. *Dalton Trans.* **2001**, *0*, 850−857.
(71) Pérez-Yáñez, S.; Castillo, O.; Cepeda, J.; García-Terán, J. P.; Luque, A.; Román, P. *Eur. J. Inorg. Chem.* **2009**, 3889−3899.
(72) Kaim, W.; Titze, C.; Schurr, T.; Sieger, M.; Lawson, M.; Jordanov, J.; Rojas, D.; García, A. M.; Manzur, J. *Z. Anorg. Allg. Chem.* **2005**, *631*, 2568−2574.